IJCRR
Vol 05 issue 14
Section: General Sciences
Category: Research
Received on: 30/11/12
Revised on: 02/01/13
Accepted on: 04/02/13

COMPARATIVE MOLECULAR MODELING STUDY OF BINDING OF MITOXANTRONE WITH D-(ATCGAT)$_2$ AND D-(CTCGAG)$_2$ HEXAMER DNA SEQUENCES

Shilpa Dogra[1], Pamita Awasthi[1], Ritu Barthwal[2]

[1]Department of Chemistry, National Institute of Technology, Hamirpur, H.P, India
[2]Department of Biotechnology, Indian Institute of Technology, Roorkee, India

E-mail of Corresponding Author: shilpadogra.84@gmail.com

ABSTRACT

Mitoxantrone (MTX) - 1, 4–dihydroxy–5, 8–bis [[2–[2–hydroxyethyl) amino] amino]–9, 10–anthracenedione is, clinically well established anthracycline class of anticancer drug. Till today no structural details confirm the interaction of mitoxantrone with its receptor site i.e. DNA Although it has been proposed and confirmed that drug binds to DNA specifically at 5'-CpG-3' site and flanking sequences play an important role. Also, functional group present on the tricyclic aromatic chromophore plays vital role in interactions. Molecular modeling tool has been applied to study binding interaction of mitoxantrone (MTX) with two hexameric DNA sequences i.e d-(ATCGAT)$_2$, d-(CTCGAG)$_2$. The electrostatic interactions play a vital role in sequence specific identification at receptor site. Study indicates the partial intercalation of mitoxantrone into 5'-CpG-3' base pair step while side chains at 5, 8 position interacts with backbone phosphate group futher stabilizes the complex. The conformation flexibility of the minimized complex is studied by backbone torsional angle as well helical parameters. It has been seen that MTX exhibit sequence specific binding. It is n+1, n+2, n+3/n-1, n-2/n-3 base pairs play important role in binding process. Studies propose the partial intercalation mode of binding.

Keywords: molecular modeling, DNA, mitoxantrone, hexamer sequences,

INTRODUCTION

Mitoxantrone (MTX), a synthetic anthraquinone drug (Fig. 1), exhibit considerable promise as an antitumor agent in the treatment of acute nonlymphocytic leukemia, advanced breast cancer, and non-Hodgkin's lymphomas[1]. Preferential accumulation of mitoxantrone in nucleoli, binding of the drug to chromatin and to cytoplasmic RNA, high affinity for DNA and RNA in solution, all points out to the fact that both DNA transcription as well as RNA processing is influenced by the drug[2, 3]. Number of mechanisms of MTX action involving formation of MTX-DNA complexes have been proposed, including trapping of the topII complex, aggregation and compaction of chromatin[4-7]. The DNA-MTX-topII cleavable complex is a reversible molecular event. It leads to cell death probably due to halting ongoing cellular processes, which ultimately trigger of the cell death program[7]. Another type of DNA damage arises probably by the formation of free radicals by MTX[8]. Evidence for intercalative binding mode of mitoxantrone to DNA has been reported by electron microscopy study[9,10]. It is very well established from several physiochemical techniques that the intercalation of mitoxantrone with cellular DNA contributes significantly towards its cytotoxic action[10-13], however the exact mode of DNA interaction at present is unclear. The experimental studies confirmed its biological effects via intercalation at 5'-CpG-3' site on DNAs followed by electrostatic cross links with DNA backbone to stabilize the process[13-15]. Recently Phillips et al. reported that the cytosine methylation enhances

mitoxantrone-DNA adduct formation and also the 3-fold enhancement in transcriptional blockage at methylated site[16].

Intercalative mode of binding of mitoxantrone to DNA has been proposed via ^{1}H and ^{31}P NMR studies[13, 17-20]. Further, computational studies indicates the pyrimidine (3'-5') purine step for preferential intercalation site for drug[21]. It is dispersion energy and electrostatic interaction which contribute towards the stability of complex[22]. Therefore, this is an important area of interest to understand the structural factors at atomic level which control the chemical recognition process via MTX at DNA. Structural tools such as X-ray crystallography and NMR spectroscopy coupled with molecular modeling technique have made considable impact on our understanding of molecular basis of drug-DNA interactions.

Therefore, in this research article we propose molecular modeling study of mitoxantrone with oligonuclotide sequences i.e d-(ATCGAT)$_2$ and d-(CTCGAG)$_2$ using MOE (molecular operating environment software tool). Our approach is to understand the molecular interactions at atomic level as proposed by various groups and further confirm the same via experimental tool. This piece of work is a part of research program undergoing our labortary on drug-DNA interaction study. Results of the present study is complied in the form of total interaction energy and structural conformation of drug as well as DNA before and after binding. We are in progress of solving the detailed structural parameters involved during MTX-DNA interactions by ^{I}H and ^{31}P NMR tool which will be repoted subsequently.

COMPUTATIONAL METHODOLOGY

Molecular operating environment (MOE) from chemical computing group, Montréal, Canada has been used for MTX-oligonucleotide interaction study. X3DNA software (downloaded from www.rutchem.rutgers.edu) has been applied for conformational analysis and vizulization of oligonucleotide sequences before and after simulations. All the simulations has been carried out on SunBlade 2500 workstation load with Sun Solaris operating system. Models of d-(ATCGAT)$_2$ d-(CTCGAG)$_2$ has been generated using "Create Sequence" panel of Builder module. Similarly Builder and Editor module is applied for construction of mitoxantrone model followed by energy minimization protocol to set up atomic coordinates with least potential energy. Non-linear optimization technique is used to determine the atomic position. MMFF94x force field is used for potential set up on atoms[23].

$E_{Total} = E_{str} + E_{ang} + E_{stb} + E_{oop} + E_{tor} + E_{vdw} + E_{ele} + E_{sol} + E_{res}$

All bonded, Van Der Waal's, electrostatic and restrained energy forms were enabled. Distance dependant dielectric constant was fixed at 1.0 alongwith cut off value for non-bonding interactions at 8.0. The temperature of the medium was keep at 300 K through out as explicit water salvation model has been followed in order to impass realistic approach. All bonds involving hydrogen atoms and lone pairs are constrained and all water molecules have been treated as rigid bodies. NVT (where N = number of particles, V = volume, T = Temprature) statistical ensamble has been specified for molecular dynamics simulations. Duration of simulations was fixed as 100 ps with 0.5 ps time step. In totality 200 structures were saved at regular interval of 0.5 ps. The trajectory of 200 structure were saved in dynamics trajectory database (*mdb). Data base browser of the MOE software used to visualize the trajectory. Same protocol is followed for all molecules i.e oligonucleotide alone as well as complex. Minimum energy conformations of DNA alone as well as in complex mode with MTX has been chosen for further analysis.

The interaction energy (E_I.E) of both the complxes is calculated using[24,25] eq. (1)

E_I.E = E_T.E – (E_drug + E_Oligo)

Where E_T.E = total potential energy of the complex, E_drug = energy term for mitoxantrone and E_Oligo = energy term for oligonucleotide sequences.

Focus on E_tor, E_vdw and E_electrostatic as they are considered to be major contributors towards interaction between MTX and oligohexanucleotide. The conformational changes at structure of oligonucleotide before and after simulation in alone and complex mode has been studied deeply via X3DNA software.

RESULTS AND DISCUSSION

Drug-DNA Binding Study

Energy profile and H-bonding interaction study

The comparative energy analysis of binding of MTX to DNA hexamer sequences i.e d-(ATCGAT)$_2$ and d-(CTCGAG)$_2$ has been carried out. MTX has been allowed to place itself at 5'-C3pG4-3' base pair step at both hexamer DNA sequences. The total energy, interaction energy and other fragment of energy i.e torsion energy and van der waal's energy has been tabulated in Table 1. The total energy of both the hexameric sequences goes more negative upon binding to MTX which demonstrate the stabilization of complexes. Rise in interaction energy up to 143.54 kcal/mol has been observed in case of MTX-CTCGAG complex. Not much of the difference could be seen in case E_vdw while E_tor is on rise and E_elc. is going more negative in case of MTX- CTCGAG complex (Table 1).

Hydrogen bonding/electrostatic interactions between MTX and oligonucleotide are an important area of study. We have observed few common and some additional interaction between drug atoms and DNA bases. Common interaction site for both the complexes is phosphate group at T2pC3 and T3pC9 steps where as in MTX-ATCGAT complex, 12NH at side arm of MTX forming hydrogen bond with N7 of G4 residue while 1OH group of MTX is interacting oxygen atom of sugar molecule at G4 base (Fig. 2). This observation is in accordance to the experimental results based on DNA foot printing study confirms the role played by 1OH/4OH groups at C1 and C4 position of anthraquinone chromophore in recognition of preffered nucleotide sequences and further flanking base pairs at n+1/n-1 or n+2/n-2 do play role in recognition[26]. On replacing A1 base by C1 in case of d-(CTCGAG)$_2$ hexameric sequences, though interaction energy going up which means gap between drug-DNA is on rise. Rise in gap leads to destabilization of the complex and at the same time important interaction between 1OH at C1 with base pair sugar molecules is also missing. But if we go through the energy profile i.e E_tor which is on rise while E_elc is coming down in comparison to MTX- ATCGAT complex.

Conformational changes in DNA

Sequence specific protein/ligand interactions with DNA unambiguously depends upon the DNA conformation/configuration i.e DNA base pairs, flanking sequences, sugar-phosphate backbone etc. This explains the relative significance/ importance of each of these interactions on the structure and function of DNA. We have chosen two oligonucleotide and observed the difference in interactions energy and also interms of interatomic interaction in complex using semi-empicical model. Idea is to explore the difference in change in DNA conformations at sugar-phosphate backbone, inter-intra base pair interactions.

DNA Backbone torsional angle study

Backbone torsional angles for d-(ATCGAT)$_2$, d-(CTCGAG)$_2$ (alone) and MTX-ATCGAT, MTX-CTCGAG complexes has been analyzed using X3DNA software. Torsion angles along the backbone of the oligonucleotide are defined as P – α- O5' – β- C5' – γ- C4' – δ- C3' – ε- O3' – ζ- P and χ is glycosyl angle. For a nucleotide in a B-DNA conformation, the phosphate groups are normally found in gauche, gauche (g,g) conformation, whereas after interacting with

drug molecules they transform into gauche, trains (g,t) conformation. This transition from g,g to g,t on intercalation of drug chromophore is associated with opening of adjacent base pairs at intercalation site. It is observed in the complex of MTX- ATCGAT, angle alpha (α) through zeta (ζ) show variations with base residues. The angle α varies in a range -50° to -90° except for A11 residue where value has been increased to trans conformation. The angle beta (β) shows appreciable variations and adopts trans conformation for all the residues. The variation of gamma (γ) is in the range 50-82° and adopt gauche+ conformation for all the residues. Delta (δ) angle, which is known to be correlated with sugar pucker remain in the region C2'-endo pucker having value ~150° except for T12 and C9 residues. Epsilon (ε) angle adopt trans conformation except for G10 residue where value is found to be gauche- conformation. Zeta (ζ) angle show fluctuations from B-DNA structure and large variation has been observed for T2 and G4 residues. Sugar pucker and glycosidic torsional angles are typical parameters that define the geometry of nucleotide. It is observed the glycosidic angle (χ) are in medium anti conformation range for C3/G10 and G4/C9 residues whereas for all other residues it is in high anti range as typically found in B-DNA[27]. The P value lies in the range of 116-190° while exception has been observed for T12 residue. C9 residue has minimum P value (116°) while C3 residue has a maximum value (189°). Overall Pseudorational phase angle adopts a favorable S conformation (Table 3).

Similarly it has been observed in MTX-CTCGAG complex, angle alpha (α) through zeta (ζ) show variations with base residues. Alpha (α) angle fall within the range of B-DNA with little flucuation in value has been observed for A5 residue. The angle beta (β) shows the variation specifically for middle residues, but overall it adopts trans conformation. Gamma (γ) value lies in the range of 50-67° and adopt gauche$^+$ conformation, characteristic of B-DNA[27]. Delta (δ) angle adopt trans conformation for all the residues and not much variation has been observed. Epsilon (ε) angle shows fluctuations at intercalation site i.e C3/G4. Exception behavior in Zeta (ζ) angle has been observed for terminal thymine residues i.e T2 and T8. Glycosidic angle (χ) is in medium anti conformation range and Pseudorational phase angle adopts a favorable S conformation for all the residues.

Values for all the backbone torsional angles α, β, γ, δ, ε, ζ as well as χ and P are near to B-DNA structure that means B-DNA geometry remain maintained throughout the simulations. Little variation in α i.e A1pT2:A11pT12 (trans) for d-$(ATCGAT)_2$ and C1pT2:A11pG12 (gauche) for d-$(CTCGAG)_2$ respectively, ε at C3pG4:C9pG10 step is trans for d-$(ATCGAT)_2$ and gauche for d-$(CTCGAG)_2$. Also ζ showed little fluctuation at both the nucleotides.

Helicoidal Parameters

The complete DNA conformation thus obtained has been described in terms of helicoidal parameters, which describe the conformation of the nucleotide pairs within the duplex. Intra base pair parameters shear, stretch, stagger, buckle, propeller and opening values for both complexes as calculated and compared to the B - DNA structure (Table 4).

In MTX-ATCGAT complex, shear, stretch and stagger show significant variation and maximum deviation has been observed in the terminal base pairs. Buckling angle also shows variations and large buckling has been observed for above and below the intercalation site. Propeller and opening values also show fluctuations for all the base pairs. Maximum propeller value has been observed in terminal base pairs and on the other hand maximum opening value is observed at intercalation site.

In MTX-CTCGAG complex, shear, stretch and stagger values show variation along the base steps. But not much deviation as in MTX-ATCGAT complex has been observed. Buckling

angle show fluctuations and maximum buckling have been observed in terminal base pairs. This could be due to intercalation of MTX at the central base pair, affecting the flaking base pairs. Propeller and opening base also show fluctuations. But in this complex, opening value for central base pair is not much larger as in case of MTX-ATCGAT complex.

Similarly inter base pair parameters shift, slide, rise, tilt, roll and twist values are tabulated (Table 5). In MTX-ATCGAT complex; shift does not show significant variation from B-DNA structure. Slide is maximum for central base pair step C3pG4:C9pG10 and minimum for terminal step. The rise per residue lie in the range of 3.2-4.0 A° except for a central base pair, it is 7.04 A° almost double to other base pair as expected for intercalation cavity. The tilt angle shows large fluctuations and maximum values are observed for T2pC3/G10pA11 step. The roll angle is negative for all the base pairs. The negative roll value indicates widening of major groove and narrowing of the minor groove. Twist angle for all the base pairs lie in between 30-37° except for T2pC3/G10pA11 step, here value is increased to ~50°. This means large negative roll value for T2pC3/G10pA11 step is compensated by large positive twist value.

On the other hand in MTX- CTCGAG complex, shift and slide value show variations, maximum shift value is observed for C1pT2/A11pG12 step and maximum slide value is observed for central step C3pG4/C9pG10. Like that in MTX-ATCGAT complex, rise value for central step is also increased, almost double to the other base pair. This means that MTX make a cavity for intercalation. Variation has been observed for tilt and roll value. Twist value has been observed in between 30-38°, almost compatible with B-DNA.

CONCLUSION

It is well established that base pair stacking interactions as well as hydrogen bonding interactions between base pair, hydrophobic-hydrophillic interactios between sugar and phosphate backbone add on to the stability of the DNA and the interaction site for all proteins and ligands. 5'-pyrimidine-purine-3' is well established intercalation site and 5'-CpG-3' step is the confirmed step where mitoxantrone is considered to be steping in. Theoretically using semi-emperical mode of calculations, we propose that it is not only n+1 & n-1 step but n+2, n+3 & n-2, n-3 step do effect the binding process and dictates the binding mechanism and overall stability of the complex as suggested by Phillips et al. 2004. We have chosen two hexanucotides sequences i.e d-$(ATCGAT)_2$ and d-$(CTCGAG)_2$ where 'TCGA' step is common. Interestingly, before binding both the hexanucleotide sequences posses equal total potential energy. After interacting with mitoxantrone, d-$(ATCGAT)_2$ sequence considred to be better over d-$(CTCGAG)_2$ sequence in terms of interactions energy. Conformational analysis of drug before and after explains two extended arms of drug fanning towards 5' and 3' end of the oligonucleotide sequence as proposed by NMR and other experimental models[13,22]. We allowed MTX molecule to move through major groove as major groove binding mode was proposed[13,23]. N2 and N7 position on guanine at intercalation site are very important for MTX interactions as it has been considered to be absolute requirement for MTX-DNA stable complex formation, experimentally. Mitoxantrone posses NH and OH functional groups which favours hydrogen bonding with hydrogen acceptor region at the DNA major and minor groove. Experimentally it is well explained the involvement of 12NH, 14OH, 1OH, 4OH and 11NH group of MTX with exocyclic amino, oxo and endocyclic hetero atoms at the intercalation cavity[23] i.e CpG.

On comparing the experimental data from literature and data generated from our model, it has been observed that terminal 14OH of the mitoxantrone show common hydrogen bond interactions with phosphate of $T2_PC3$ step while

12NH-N7G4 and 1OH-O'G4 interactions are observed in d-(ATCGAT)$_2$ complex. These two H-bonding interctaions has been observed experimentally as well[20]. Also Phillips et al. 2004 model proposes the same. Therefore, as per sequence dependence interactions, DNA conformation/configuration play major role towards this. To confirm this we carried out detail DNA conformational analysis. T2pC3/G10A11 is a common base pair step in both oligonucleotide sequences. Twist angle is 50.75° in case of d-(ATCGAT)$_2$ sequence, which is very high in comparison to B-DNA sequence. At the same time no such observation has been encountered in d-(CTCGAG)$_2$ sequence. 14OH of mitoxantrone is interacting with phosphate group of T2pC3 step in both the sequences. As per quantum mechanical study on stacking interactions and the twist angle of the DNA variation in DNA twist parameters could be due to the stacking interactions involving steric repulsion between exocyclic groups of nucleotide in minor and major groove and π-π interactions between the base[28]. Before interactions of MTX to d-(ATCGAT)$_2$ and d-(CTCGAG)$_2$ hexanucleotide, twist angle show small variations. For B-DNA the twist anglen fall in the range 32-36°. But upon complex formation twist angle of C3pG4:C9pG10 of both the hexanucleotide having a value 28.9° and 32.42° for d-(ATCGAT)$_2$ and d-(CTCGAG)$_2$ respectively. For d-(CTCGAG)$_2$ it is close to B-DNA and did not observed any fluctuations at n+1, n-1 & n+2 step, but changes observed at n-2 step. In case of d-(ATCGAT)$_2$ huge variations has been seen at T2pC3:G10pA11 step. Therefore, interbase pair interactions above and below the binding step are the markers for ligand binding and can be a guiding force. We could not observed the uniform pattern for intra base pair interaction in both the cases i.e d-(ATCGAT)$_2$ and d-(CTCGAG)$_2$ sequences as expected. Simultaneously, backbone torsional angles do vary in both the model in comparison to standard B-DNA model.

REFERENCES

1. Murdock KC, Child RG, Fabio PF, Angier RB, Wallace TE, Durr FE, and Citarella RV, Antitumor Agents. 1, 4 Bis–[aminoalkyl) amino]–9,10 anthracenedione. J. Med. Chem., 1979, 22, 1024–1030.
2. Feofanov A, Sharonov S, Kudelina I, Fleury F, Nabiev I, Localization and molecular interactions of mitoxantrone within living K562 cells as probed by confocal spectral imaging analysis. J. Biophys., 1997, 73, 3317–3327.
3. Feofanov A, Sharonov S, Kudelina I, Fleury F, Nabiev, I, Quantitative confocal spectral imaging analysis of mitoxantrone within living K562 cells: intracellular accumulation and distribution of monomers, aggregates, naphtoquinoxaline metabolite, and drug-target complexes. J. *Biophys*., 1997, 73, 3328–3336.
4. Smith PJ, Morgan SA, Fox ME, Watson JV, Mitoxantrone-DNA binding and the induction of topoisomerase II associated DNA damage in multi-drug resistant small cell lung cancer cells. Biochem. Pharmacol., 1990, 40, 2069-2078.
5. D'Arpa P, Liu LF, Topoisomerase-targeting antitumor drugs. Biochem. Biophys. Acta. 1989, 989, 163-177.
6. Kapuscinski J, Darzynkiewicz Z, Relationship between the pharmacological activity of antitumor drugs Ametantrone and mitoxantrone (Novatrone) and their ability to condense nucleic acids. Proc. Natl. Acad. Sci., 1986, 83, 6302-6306.
7. Parker SB, Cutts MS, Cullinane C, Phillips RD, Formaldehyde activation of mitoxantrone yields CpG and CpA specific DNA adducts**.** Nucleic. Acids Res., 2000, 28, 983–989.

8. Tarasiuk J, Tkaczyk-Gobis K, Stefanska B, Dzieduszycka M, Priebe W, Martelli S, Borowski E, The role of structural factors of anthraquinone compounds and their quinone-modified analogues in NADH dehydrogenase-catalysed oxygen radical formation. Anticancer Drug Des., 1998, 13, 923–939.
9. Lown JW, Hanstock CC, Bradley RD, Douglas GS, Interactions of Antitumor agents Mitoxantrone and Deoxyribonucleic Acids studied by electron Microscopy. Molecular Pharma., 1983, 25, 178–184.
10. Lown JW, Morgan AR, Yen Shau–Fong, Wang Yueh–Hwa, Wilson WD, Characterization of binding of the anticancer agents mitoxantrone and ametantrone and related structures to deoxyribonucleic acids. Biochemistry. 1985, 24, 4028–4035.
11. Tanious FA, Jenkins TC, Neidle S, Wilson WD, Substituent position dictates the intercalative DNA–Binding mode for anthracene 9, 10–dione antitumor drugs. Biochemistry, 1992, 31, 11632–11640.
12. Kapuscinski J, Darzynkiewicz Z, Interactions of antitumor agents ametantrone and mitoxantrone (novantrone) with double–stranded DNA. Biochem Pharmacol., 1985, 34, 4203–4213.
13. Lown, JW, Hanstock CC, High field ^{1}H–NMR analysis of the 1:1 intercalation complex of the antitumor agent mitoxantrone and the DNA duplex [d(CpGpCpG)]. J. Biomol. Struct. Dyn., 1985, 2, 1097-1106.
14. Kotovych, G, Lown JW, Tong KPJ, High field ^{1}H and ^{31}P NMR studies on the binding of the anticancer agent mitoxantrone to d–$[CpGpApTpCpG)_2$. J. Biomol. Struct. Dyn., 1986, 4, 111-125.
15. Panousis C, Phillips DR, Sequence specificity of Mitoxantrone. Nucleic Acids Res., 1994, 22, 1342–1345.
16. Parker SB, Cutts SM, Phillips RD, Cytosine Methylation Enhances Mitoxantrone-DNA Adduct Formation at CpG Dinucleotides. J Biol. Chem., 2001, 276, 15953-15960.
17. Davies DB, Veselkov DA, Evstigneev MP, Veselkov AN, Self–association of the antitumour agent novatrone (mitoxantrone) and its hetero–association with caffeine. J Chem. Soc. Perkin Trans, 2001, 2, 61–67.
18. Davies DB, Veselkov DA, Djimant LN, Veselkov AN, Hetero–association of caeffine and aromatic drugs and their competitive binding with DNA oligomer. J Eur. Biophys. 2001, 30, 354–356.
19. Veselkov AN, Evstigneev MP, Vysotskii SA, Veseklov DA, Davies DB, Thermodynamic analysis of interaction of antibiotic mitoxantrone with tetranucleotide 5'–d (TpGpCpA) in aqueous solution based on ^{1}H NMR spectroscopy data. Biofizika 2002, 47, 432–438.
20. Zheng S, Chen Yu, Donahue CP, Wolfe MS, Varani G, Structural basis for stabilization of the tau pre-mRNA splicing regulatory element by novatrone (mitoxantrone). Chem Biol., 2009, 16, 557-566.
21. Chen XK, Gresh N, Pullman B, Nucl. A theoretical investigation on the sequence selective binding of mitoxantrone to double–stranded tetranucleotides. Nucleic Acids Res., 1986, 14, 3799-3812.
22. Riahi S, Ganjali RM, Dinarvand R, Karamdoust S, Bagherzadeh K, Norouzi PA, Theoretical Study on Interactions Between Mitoxantrone as an Anticancer Drug and DNA. Chem. Biol. Drug Des., 2008, 7, 474–482.
23. Parker BS, Buley T, Evinson B, Cutts SM, Neumann GM, Iskander MN,. Phillips DR, Molecular understandings of mitoxantrone–DNA adduct formation: Effect of cytosine methylation and flanking sequences. J Biol. Chem., 2004, 279, 18814–18823.

24. Rehn C, Pindur U, Model Building and Molecular Mechanics Calculations of Mitoxantrone-Deoxytetranucleotide Complexes: Molecular Foundations of D N A Intercalation as Cytostatic Active Principle. Monatsh chemie., 1996, 127, 631-644.
25. Awasthi P, Dogra S, Awasthi LK and Barthwal R, Software Tools and Algorithms for Biological System, Advances in Experimental Medicine and Biology, in: H.R Arabnia and Q.-N. Tran (eds.), New York, Springer, 2011, 39, 385-400.
26. Bailly C, Routier, S, Bernier J. -L and Waring M. J, DNA recognition by two mitoxantrone analogues: influence of the hydroxyl groups. FEBS Letters, 1996, 379 269-272.
27. Schneider B, Neidle S, Berman HM, Conformations of the sugar-phosphate backbone in helical DNA crystal structures. Biopolymers, 1997, 42, 113-124.
28. Lam, S. L. and Au-Yeung, S. C. F. Sequence-specific Local Structural Variations in Solution Structures of d(CGXX0CG)$_2$ and d(CAXX0TG)$_2$ Self-complementary Deoxyribonucleic Acids. J. Mol. Biol., 1997, 266, 745-760

Table 1 Energy terms (Kcal mol^{-1}), with respect to atomic coordinates for one minimized structure.

oligonucleotide alone and complex	Total energy	Interaction energy	E_Vdw	E_tor	E_elc.
d-(ATCGAT)$_2$	-4534.43	-	2172.91	191.46	-7310.44
MTX- ATCGAT	-5162.20	547.74	2624.63	178.78	-8477.16
d-(CTCGAG)$_2$	-4697.92	-	2274.90	184.58	-7577.25
MTX- CTCGAG	-5182.15	691.28	2647.03	188.71	-8341.48

Table 2 Atomic interaction (A$^{\circ}$) of mitoxantrone with hexamer DNA sequences d-(ATCGAT)$_2$ and d-(CTCGAG)$_2$

Present Work				Zheng et al. 2009	
MTX- ATCGAT	Distances (Å)	MTX- CTCGAG	Distances (Å)	MTX-tau pre-mRNA	Distances (Å)
14OH- T2pC3	1.60	14OH- T2pC3	1.57	12NH-N7G17	2.5
14OH- T8pC9	1.63	14OH- T8pC9	1.65	12NH-O6G1	3.2
12NH- N7G4	2.30	-	-	11NH-O2PG6	4.2
1OH- O1'G4	1.65	-	-	11NH-O6G1	2.8
				14OH-O1PG1	3.0
				1OH-O1'G4	2.2
				4OH-O2'A2	2.2

Table 3 Backbone torsional angles, pseudoratation phase angle and glycosidic bond rotation of the final structure in degrees analyzed using X3DNA program.

		α		β		γ		δ	
ATCGAT-MTX									
Strand I	Strand II	Strand I	Strand II	Strand I	Strand II	Strand I	Strand II	Strand I	Strand II
A1	T12	…	-69.7	-172.8	-175	54.9	46.3	158.6	77.1
T2	A11	-51.4	-157.7	166.2	-162.4	46.9	82.4	161	152.6
C3	G10	-72.6	-65.1	154	153.2	53.7	61.5	149.2	152.7
G4	C9	-84.7	-91.0	165.2	-179.0	60.2	50.3	157	112.6
A5	T8	-62.5	-70.7	137.1	-178.5	70.6	66.1	141.6	145.4
T6	A7	-64.4	….	179.3	170.8	64.4	61.8	128.9	154
CTCGAG-MTX									
C1	G12	….	-62.4	168.1	175	49.9	55.7	144.6	126.5
T2	A11	-60.6	-68.1	168.8	154	55.3	67.8	145.1	145.6
C3	G10	-72.9	-71.6	176	140.8	53.6	61.9	116.7	153.1
G4	C9	-67.9	-70.9	132.8	177.4	60.8	59.3	155.9	118.2
A5	T8	-84.1	-57.2	153.8	156.4	44.1	56	143.3	145
G6	C7	-65.3	---	176.2	168.4	58.4	51.2	116.7	146.4
B-DNA		-63		136		54.0		123	

		ε		ζ		χ		P	
Strand I	Strand II	Strand I	Strand II	Strand I	Strand II	Strand I	Strand II	Strand I	Strand II
ATCGAT-MTX									
A1	T12	-160.8	…	-128.1	….	-103.9	-151.3	178.3	35.1
T2	A11	-114.1	-174.9	-175.2	-95.5	-102.1	-115.4	162.4	182.5
C3	G10	-122.5	-53.8	-107.6	94.1	-88.9	-90.5	189	168.3
G4	C9	-138.8	-123.5	154.3	112.6	-69.1	-95.7	158	116.9
A5	T8	178.1	-167.5	-89.8	-69.6	-120.1	-129	170.4	158.1
T6	A7	….	-170.4	….	-102.3	-144.8	-145.1	123.4	175.2
CTCGAG-MTX									
C1	G12	-152.5	---	-131.7	---	-130.9	-125.5	159.5	132.2
T2	A11	-168.6	-165.6	-87	-100.1	-112.6	-130.3	159.8	165.1
C3	G10	-92.8	-158.2	-175.8	-153.5	-121	-102.6	116.1	168.2
G4	C9	-96	-98.3	162.3	-173.7	-95.6	-126.7	165.3	119.7
A5	T8	-170.9	-171.8	-92.6	-88.3	-121.3	-118.3	157.2	156.6
G6	C7	---	-144.8	---	-156.5	-130.4	-127.1	119.6	156.9
B-DNA		-169		-108		-105		162	

Table 4 Helical intra parameters for mitoxantrone with d-(ATCGAT)$_2$ and d-(CTCGAG)$_2$ hexamer DNA sequences.

Step	Shear(A◦)	Stretch(A◦)	Stagger(A◦)	Buckle(deg)	Propeller(deg)	Opening(deg)
MTX- ATCGAT Complex						
A1-T12	0.2	0	1.28	14.94	5.72	-11.3
T2-A11	0.57	-0.18	0.89	15.89	-15.57	-20.12
C3-G10	0.57	0.07	0.22	17.37	-4.99	12.78
G4-C9	-0.08	-0.13	-0.17	-10.04	5.06	2.35
A5-T8	0.85	-0.03	0.24	-1.13	-5.78	-8.77
T6-A7	-0.08	-0.16	0.44	-14.61	3.88	-13.6
ave.	0.34	-0.07	0.48	3.74	-1.95	-6.44
MTX- CTCGAG Complex						
C1-G12	0.21	-0.26	-0.09	5.48	-1.48	-4.97
T2-A11	-0.97	0.28	-0.01	10.91	-5.7	-16.92
C3-G10	0.42	-0.35	-0.17	12.19	5.58	-1.15
G4-C9	-0.51	-0.33	-0.15	-3.56	5.48	0.15
A5-T8	0.52	0.21	-0.35	-0.06	-8.87	-22.25
G6-C7	-0.36	-0.31	-0.06	2.34	9.32	-2.03
ave.	-0.11	-0.13	-0.14	4.55	0.72	-7.86
B-DNA	0	0	0.02	0	3.6	-4.1

Table 5 Helical inter parameters for mitoxantrone with d-(ATCGAT)$_2$ and d-(CTCGAG)$_2$ hexamer DNA sequences

Step	Shift(A°)	Slide(A°)	Rise(A°)	Tilt(deg)	Roll(deg)	Twist(deg)
ATCGAT-MTX Complex						
A1T2/A11T12	0	-1.64	3.74	0.78	-10.06	31.46
T2C3/G10A11	2.27	1.08	3.78	12.14	-34.24	50.75
C3G4/C9G10	0.31	2.42	7.04	4.96	-8.15	28.93
G4A5/T8C9	-1.97	-0.02	3.27	-1.41	-1.46	37.13
A5T6/A7T8	0.24	-1.9	4.02	-1.61	-11.65	30.45
ave.	0.17	-0.01	4.37	2.97	-13.11	35.75
CTCGAG-MTX Complex						
C1T2/A11G12	-1.16	-0.99	3.75	-1.63	-18.03	31.62
T2C3/G10A11	1.97	-0.52	3.59	0.9	-5.33	38.61
C3G4/C9G10	0.78	2.14	6.57	1.76	-32.74	32.42
G4A5/T8C9	-2.33	-0.71	3.51	-0.08	-7.19	38.91
A5G6/C7T8	2.29	-1.07	3.86	-0.73	-20.73	29.89
ave.	0.31	-0.23	4.26	0.04	-16.8	34.29
B-DNA	0	0	3.4	0	0	36.0

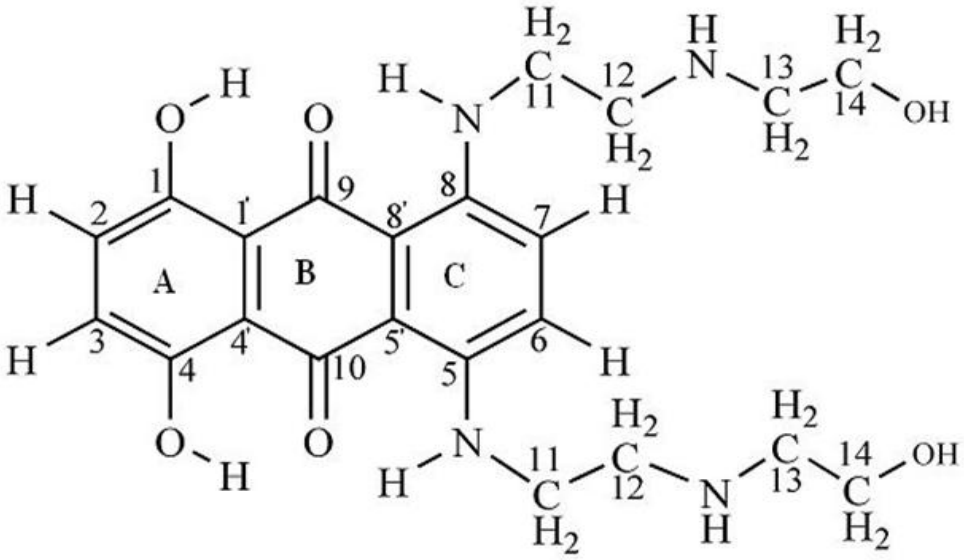

Figure 1 Chemical Structure of mitoxantrone (abbreviated MTX)

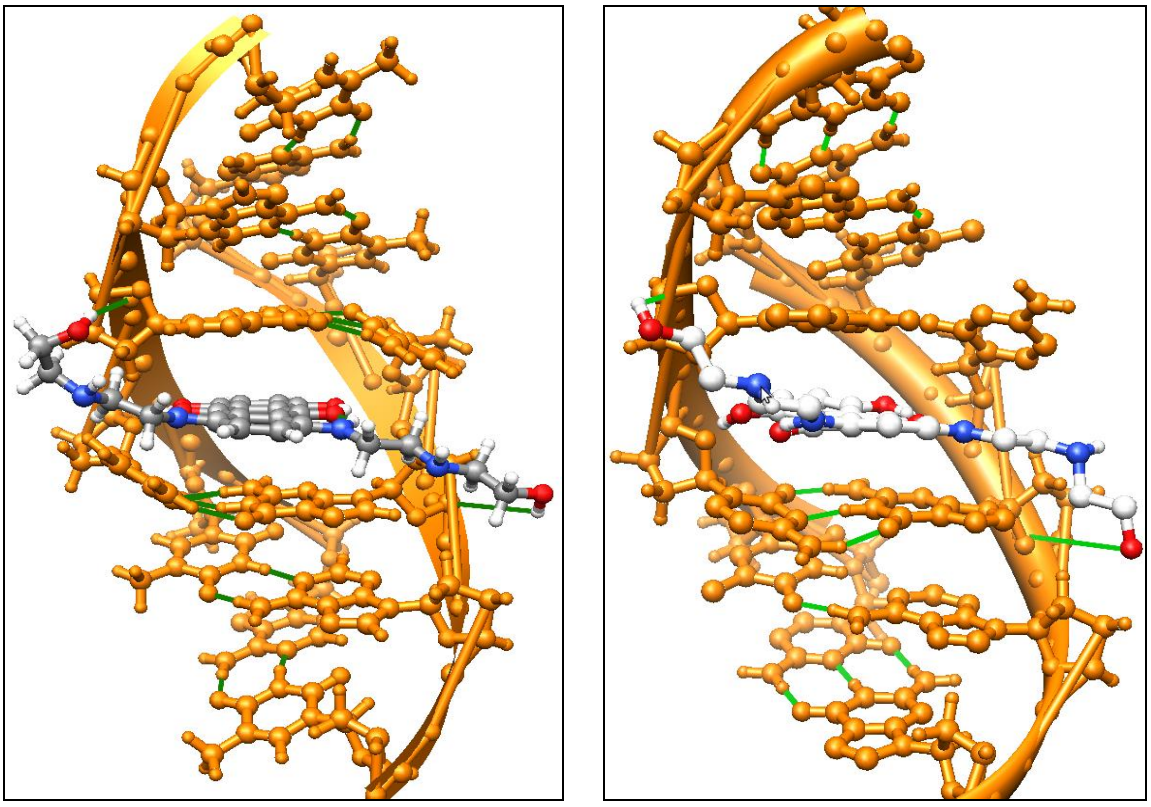

(a) (b)

Figure 2 Sterioview of minimized complex of (a) ATCGAT-MTX (b) CTCGAG-MTX. The figure depicts the DNA helical structure in brown color and MTX in gray color. The drug molecule interacting with backbone of DNA is depicts in green color.